MEASURE OF FRACTURE TOUGHNESS IN COMPOSITE STRUCTURES USING INFRARED THERMOGRAPHY

Teddy LISLE[1], Natthawat HONGKARNJANAKUL[1], Christophe BOUVET[1], Marie-Laetitia PASTOR[1], Philippe MARGUERES[1], Samuel RIVALLANT[1]

1 : Université de Toulouse ; INSA, UPS, Mines Albi, ISAE ; ICA (Institut Clément Ader)
ISAE (Institut Supérieur de l'Aéronautique et de l'Espace)
10, avenue Edouard Belin, -BP 54032- 31055 Toulouse cedex 4
e-mail : christophe.bouvet@isae.fr

Keywords: infrared thermography, fracture toughness, composite fracture

Abstract
Fracture toughness is one of the most important properties of any material for a lot of design applications involving damage and crack growth. Unfortunately its value can be difficult to evaluate with standard methods such as "compliance" method. In this work, two special cases have been studied and infrared thermography has been used to overcome the limitations of conventional methods.
Damage of compressive fiber failure in unidirectional composite laminate has been chosen due to its difficulty to evaluate toughness. The infrared thermography has been used to follow compressive failure mode developing during an indentation test and a compression after impact test, and to evaluate the fracture toughness of compressive fiber failure.

1. Introduction

The studied cases deal with the compressive fiber failure mode in laminated composites [1]. This failure mode is known as a very complex mode occurring as a result of the kinking process. Currently, no standard tests are available to determine the fracture toughness of this phenomenon. Infrared thermography has been used to follow compressive failure mode developing during an indentation test and a compression after impact test, and to evaluate the fracture toughness of compressive fiber failure.
From the past 20 years, infrared thermography has been widely used to study the dissipative phenomena in materials, such as plasticity in metals [2-3] or damage in polymers [4]. Using the framework of irreversible thermodynamics, Chrysochoos et al. [5] have presented a methodology to estimate the internal heat sources associated with the dissipative phenomenon from temperature measurement on the sample surface. Nevertheless, the use of infrared thermography to study dissipated thermal energy is quite recent in composite materials and is essentially applied to fatigue loading. For example, Naderi et al. [6] used infrared thermography to characterize damage stage evolution by calculating the dissipated heat during fatigue loading of thin woven laminates. Nevertheless, using crack tip contour integral analysis [7], Freund and Hutchinson [8] and Soumahoro [9] have shown that the fracture toughness is linked to dissipative work. In addition, since the early work of Taylor and

Quinney [10], it is well known that dissipative work is mainly converted into heat in metallic [11] and polymeric materials [12].
Hence, in this study we propose linking the fracture toughness to the experimental heat sources [13]. In this way, the fracture toughness can be computed even for experiments where the stiffness variation remains small.

2. Compressive fiber failure toughness in unidirectional laminated composite

The characteristic of fiber compressive failure is usually considered as a complex failure mode [1, 14]. Furthermore, the critical energy release rate in compression, G_{Ic}^{comp} (generally referred to mode I intralaminar fracture) is even more complex. Different approaches have been proposed in the literature to determine this value. For example, Pinho et al. [1] used compact compression (CC) tests to evaluate the fibre G_{Ic}^{comp} of T300/913 carbon/epoxy laminates. Initiation toughness value for kink-band formation was obtained equal to 79.9 N/mm, whereas the propagation was not reliable due to an appearance of other failure modes such as crushing or delamination. Soutis and Curtis [14] also measured the G_{Ic}^{comp} of T800/924C carbon/epoxy $[0,90_2,0]_{3s}$ UD laminates. The values calculated by analytical formulations based on elastic laminated properties were determined to be equal to ≈34-39 N/mm. The two studies show clearly the difficulty to evaluate the compressive fiber fracture toughness.
The first step to evaluate G_{Ic}^{comp} is to choose the appropriate test. The test should promote compressive fiber failure as pure and stable as possible. In fact it is almost impossible to exhibit only compressive fiber failure because it is a very complex failure mode which is followed by secondary failure modes such as delamination or matrix cracking. Moreover the stacking sequence has much effect on the failure mode. In fact it could be interesting to use pure unidirectional laminate to isolate the compressive fiber failure mode, but it is uncertain the failure mode is similar to this one developing in a multidirectional laminated composite. Then in this study two applications with multidirectional laminated composite have been chosen to be representative of real composite structure.
The material used in this study is a T700GC/M21 (carbon/epoxy) UD prepreg with 0.25 mm-ply thickness. The laminates are 16-ply, balanced, symmetrical and quasi-isotropic which have the total thickness of about 4 mm. They are cut into rectangular plates 100x150 mm^2 for the reason of testing on impact and CAI (compression after impact) according to the Airbus Industries Test Method (AITM 1-0010).
The first test deals with compressive fiber crack on the surface of $[90_2,0_2,-45_2,45_2]_s$ laminate during impact test [15] (Fig. 1a). Due to the short edge boundary conditions, the outermost 90°-plies are subjected to more bending rather than the inner plies. As a result, compressive influence is generated on the upper layers and compressive cracks are observed. Moreover, a static indentation test was used instead of impact test, because we need a lengthy or long time test for observing damage by using infrared thermography camera. The static indentation test (Fig. 1a) is similar to impact test: a 100x150 mm^2 rectangular plate specimen is simply supported on a 75x125 mm^2 frame. An indentor of 16 mm-diameter applies to the centre of the specimen at a displacement rate of 5 mm/min. LVDT sensor is placed to measure displacement of the crosshead. During the test, compressive cracks of 90°-plies on the upper surface near indentor
point are observed; meanwhile an infrared camera records the temperature on the expected zone of the crack appearance (Fig. 2a).
The specimen is subjected to out-of-plane load until approximately 5 mm (for a total energy of 25 J). As can be seen the force-displacement curve in figure 2a, during loading the response is not linear due to internal damage. Matrix cracking and delamination commonly

occur prior to fiber failure [15]. The damage near the surface can be detected by an infrared thermography camera, in particular the double-ply fiber compressive failure, as the post-mortem micrograph shown in figure 3a. This fiber compressive failure arises from 3.5 mm-displacement and gradually continues to propagate until the end of loading state.

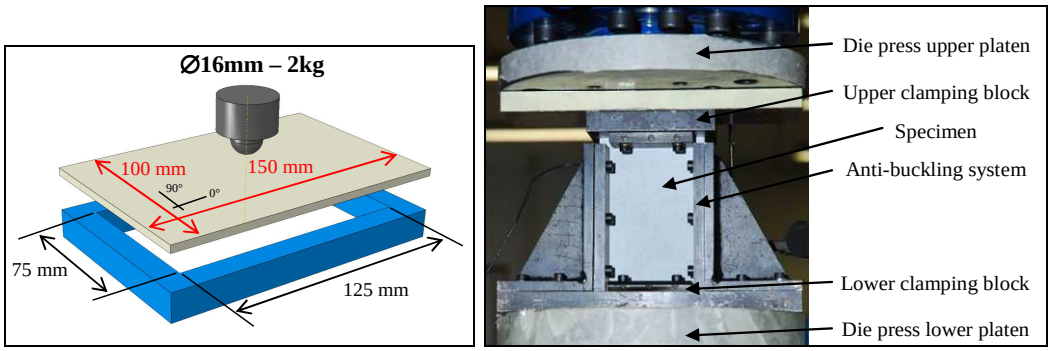

Figure 1. Experimental setup of impact/indentation test (a) and compression after impact test (b).

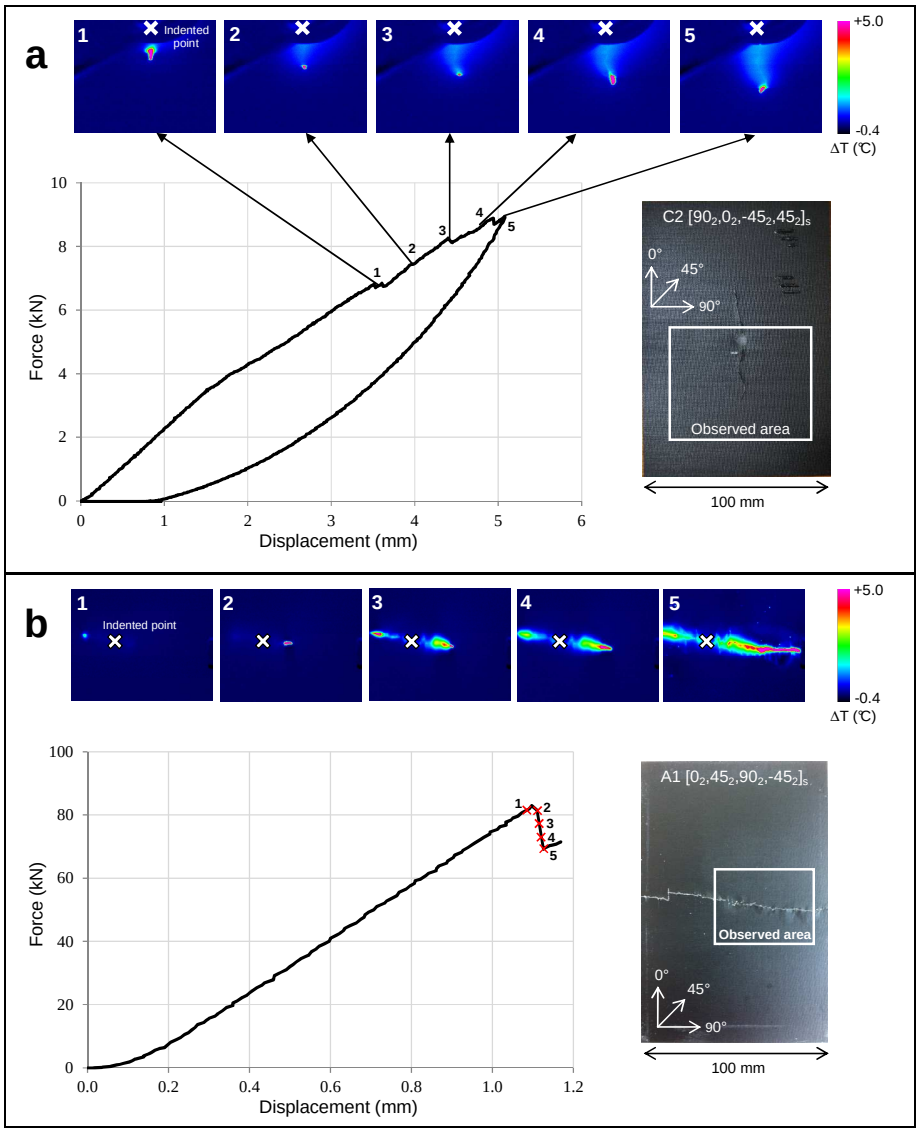

Figure 2. Damage detection by infrared thermography camera associated with force-displacement curves: static indentation test (a) and CAI test (b).

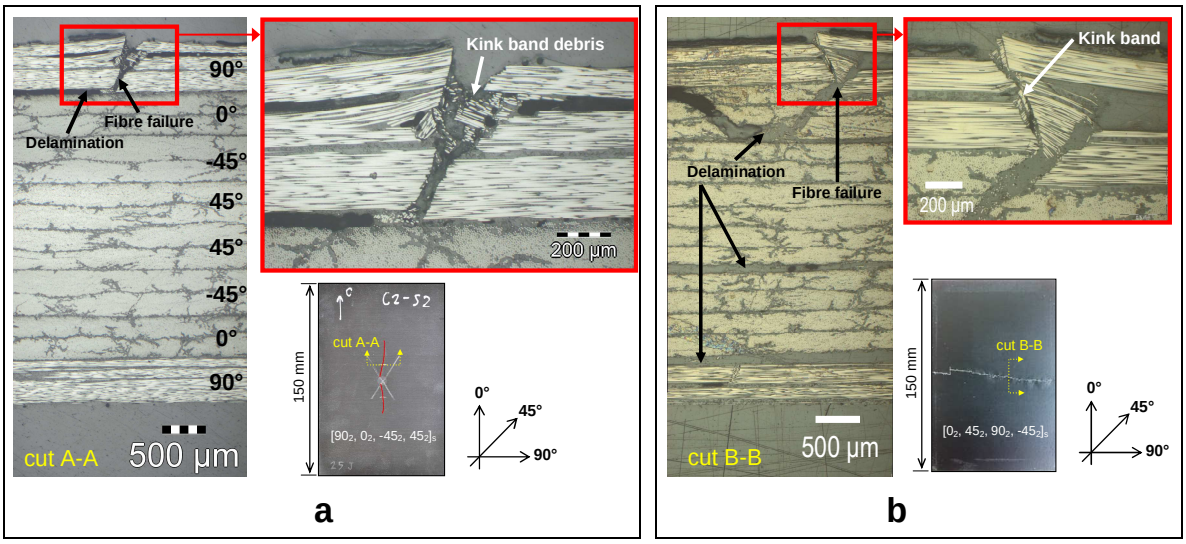

Figure 3. Post-mortem micrographs (a) static indentation test (taken from an equivalent specimen of 25 J-impact [8]) and (b) CAI test

The second test application is CAI (Fig. 1b) [16]. Failure of the outermost 0°-plies of $[0_2,45_2,90_2,-45_2]_s$ laminates, directly subjected to compressive loading, is investigated. Then, the critical energy release rate is measured based on an evaluation of the heat degradation on the observed compressive cracks. Prior to the CAI test, the plate composite laminate has been damaged by static loading in the centre of the specimen at 27.3 J-total energy [16]. Consequently, this specimen is placed inside CAI fixture and is subjected to in-plane compressive load at a displacement rate of 0.6 mm/min. An imposed displacement and a plate deflection are obtained from LVDT sensors. Thanks to the configuration of 0°-plies on the exterior, compressive failure can be easily observed. Since the CAI final failure is generally induced from the indented point, an infrared camera captures the temperature variation on the zone near this point (Fig. 2b).

During the CAI test, the force in function of displacement is relatively linear until the collapse of the specimen or final failure. The infrared thermography camera detects that the initiation of damage occurs just before the final failure. It is not clear that the damage shown at points 1-5 in figure 2b is caused by the collapse of the plate due to bending or due to the propagation of fiber cracks. However, this damage is absolutely a compressive fiber failure, as can be seen the kink bands in figure 3b. Thus, we assumed that the heat detected by thermography camera is caused by this fiber compressive failure. Note that figure 3b shows the micrograph of fiber failure mixed to other failure modes i.e. matrix cracking and delamination but it was taken after the final failure.

Both tests are operated at room temperature. An infrared camera (FLIR SC700 MW) is used to monitor the thermal response during the tests. In order to avoid thermal perturbation from the external environment, the specimens are enclosed both in a painted black box and black opaque fabric (covered outside).

The concept of determining the critical energy release rate by using infrared thermography technique is based on thermo-mechanical background. The full details can be found in [13].

When the specimen is damaged, some mechanical energy dissipation is converted to heat and can be measured by the infrared thermography camera. The critical energy release rate G_{Ic} can be estimated from the heat source ω_{hs} as:

$$G_{Ic} = \frac{1}{\beta} \cdot \frac{1}{S_f} \int_t \iint_\Omega \omega_{hs} dV dt \qquad \text{Eq 1}$$

where β represents the ratio of the energy dissipated as heat to the irreversible mechanical energy [10], S_f is the crack surface, t is the crack propagation time, and Ω is the studied domain of crack.
In the literature, the irreversible work which transforms into heat (the parameter β) may vary from 50-100% [6, 10, 13], thus an accurate estimation of energy release rates associated with crack propagation is probably uncertain and this is a debated issue for determining the value of G_{Ic} by this approach.
In this work, since the tested laminate has different plies orientation, fiber failure may damage at certain plies but not throughout the thickness of the laminate. Since the temperature field is not constant through the thickness of the laminate, solving with the 2D heat diffusion problem is not reliable. Thus, only the heat source of the compressive fiber failure cracks on the surface is considered. A 3D thermal analysis is used and the heat source function, assumed to be uniform through the damage plies, can be written as:

$$\omega_{hs} = \omega_{\max} \cdot \left[H(z-z_0) - H(z-z_1)\right] \cdot e^{-\left(\frac{(x-x_0)^2}{2\sigma_x^2}+\frac{(y-y_0)^2}{2\sigma_y^2}\right)} \cdot e^{-\left(\frac{(t-t_0)^2}{2\sigma_t^2}\right)} \quad \text{Eq 2}$$

where ω_{max} represents the maximum value of heat source, x_0 and y_0 denote the space positions associated with the global coordination x-y, and t_0 denotes the temporal position of the crack. σ_x , σ_y and σ_t are respectively the constants of the longer, larger and the propagation time of heat source, which are the optimized parameters due to ill-posed problem [13]. The term $[H(z-z_0)-H(z-z_1)]$ is the rectangular function corresponding to the crack thickness. Then, the temperature variation θ can be solved by 3D inverse heat diffusion problem:

$$\rho C \frac{\partial \theta}{\partial t} - \left[k_{xx} \frac{\partial^2 \theta}{\partial x^2} + k_{yy} \frac{\partial^2 \theta}{\partial y^2} + k_{zz} \frac{\partial^2 \theta}{\partial z^2} \right] = \omega_{hs} \quad \text{Eq 3}$$

where ρ, *C* and *k* are respectively the laminate density, the specific heat and the thermal conductivity.
From microscopic observations (Fig. 3), we assume that the temperature is uniform through the cracks thickness (the double damaged plies near the surface) and the heat source is only due to fiber compressive failure of the double-ply whereas the heat source due to matrix cracks and delamination underneath is neglected.
For numerical calculation, the solution of thermal problem is computed by using finite difference method. A small step time $\Delta t = 5.10^{-4}$ s is chosen in order to assure the convergence of results. The theoretical heat sources are determined on three different zones of each test, as shown in figure 4a for the static indentation test and figure 5a for CAI test. According to the proposed methodology [13], the optimization parameters (σ_x , σ_y , σ_t) are identified by trial-and-error method in order to correlate with the experimental temperature variation θ_{exp}.
An example of experimental-numerical correlation of static indentation test (zone 3) is presented in figure 4: Figure 4d shows the evolution of average temperature cooling in function of time. And, at temperature peak, a comparison of the temperature variation field of the crack between the experiment and the theoretical calculation is shown respectively in figures 4b and 4c; also, the evolution of temperature along X-X and Y-Y axes are presented respectively in figures 4e and 4f. As can be seen, figures 4b-4f show a good correlation between experiment and theoretical calculation after a selection of optimization parameters.
Another example of CAI test (zone 3), after the process of parameter optimization, is also presented: Figures 5b-5f show a good agreement between experimental and theoretical calculation even if an uncorrelated experimental cooling in figure 5d is found. Indeed, the instability of the evolution of experimental temperature is clearly caused by a combination of

other failure modes (delamination and matrix cracking) occurring during the crack propagation (Fig. 5b); thus precise numerical cooling cannot be obtained. Thanks to a good agreement on other factor i.e. evolution of temperature along X-X and Y-Y axes, we still rely on the chosen optimized parameters (Tab. 1).

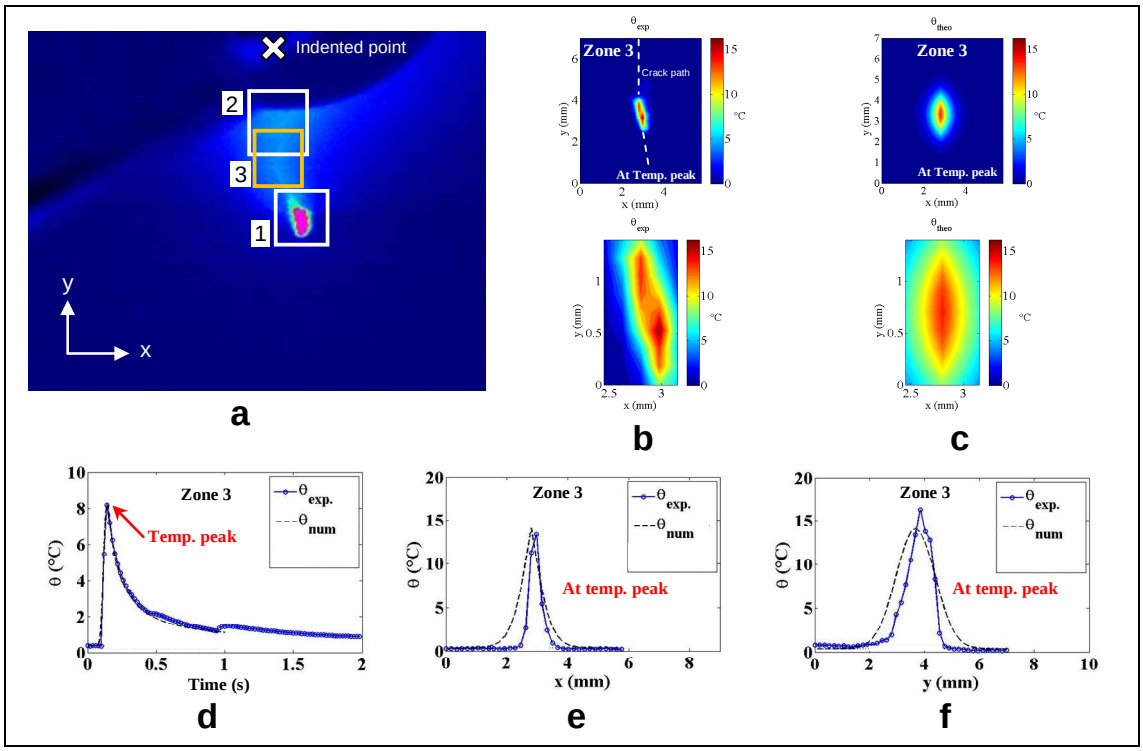

Figure 4. Evaluation of crack propagation by thermography approach from static indentation test: (a) three selected zones on experimental temperature field; (b) experimental temperature variation of crack in zone 3 at temperature peak; (c) theoretical temperature variation of crack in zone 3 at temperature peak; (d) evolution of average temperature cooling in function of time; (e) evolution of temperature along X-X axis at temperature peak; (f) evolution of temperature along Y-Y axis at temperature peak

The results above confirm that the heat sources due to plies compressive failure are well assumed by the theoretical approach for both static indentation test and CAI test, and the use of the proposed thermography methodology is applicable for UD plies. We performed on six studied zones from two different test applications. Table 1 presents the selected optimization parameters for all cases. A strange value of σ_y for CAI test in zone 1 should be noticed, that is, the high value is met. The reason is that the crack at zone 1 is caused by the specimen's collapse at final failure which does not gradually propagate like other zones.

Then, an estimation of the critical energy release rate G_{Ic}^{comp} is computed following Eq. 1. S_f denotes the crack surface and the heat source ω_{hs} is obtained thanks to the maximum value of heat source ω_{max} from the experiment and the optimization parameters previously. As mentioned before, a sensitive issue is still the ratio of the energy dissipated as heat to the irreversible mechanical energy (β). In this study, we assume this ratio, for carbon/epoxy composite, to be approximately 90% [13].

Finally, the critical energy release rate fibre G_{Ic}^{comp} can be computed [Tab. 1]. The average values of G_{Ic}^{comp} , for static indentation test and CAI test are **32.6** N/mm and **42.5** N/mm, respectively. These obtained results are well corresponding to the value found in previous work [8] (40 N/mm) from FE analysis of impact damage.

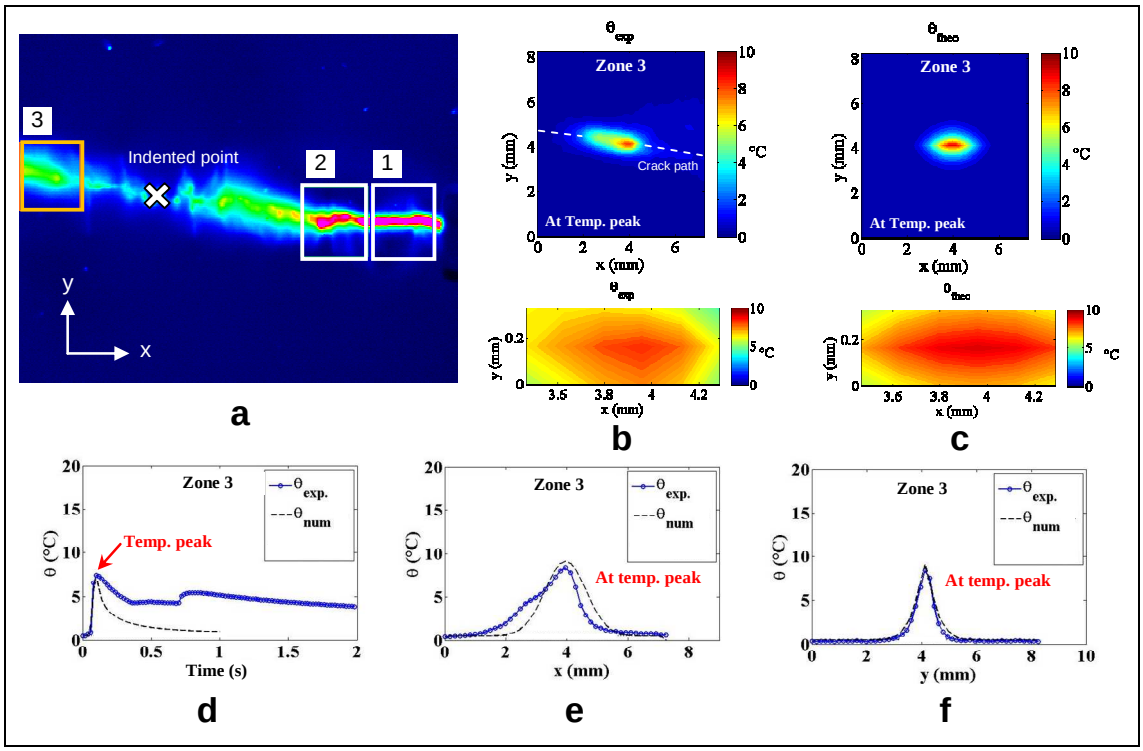

Figure 5. Evaluation of crack propagation by thermography approach from CAI test: (a) three selected zones on experimental temperature field; (b) experimental temperature variation of crack in zone 3 at temperature peak; (c) theoretical temperature variation of crack in zone 3 at temperature peak; (d) evolution of average temperature cooling in function of time; (e) evolution of temperature along X-X axis at temperature peak; (f) evolution of temperature along Y-Y axis at temperature peak

Test	Zone No.	Optimization parameters			ω_{max} (W·m^{-3})	S_f (mm^2)	$G_{Ic}^{fibre,C}$ (N/mm)
		σ_x (mm)	σ_y (mm)	σ_t (s)			
Static Indentation	1	0.083	0.990	12 e-3	2.80 e9	0.963	**39.7**
	2	0.041	0.825	10 e-3	3.50 e9	0.525	**31.6**
	3	0.041	0.660	12 e-3	2.55 e9	0.438	**26.6**
CAI	1	16.50	0.248	12 e-3	1.40 e9	3.220	**40.8**
	2	0.866	0.083	12 e-3	2.05 e9	0.495	**43.9**
	3	0.660	0.041	12 e-3	1.75 e9	0.165	**42.9**

Table 1. Values of theoretical heat source parameters obtained for the three zones of each test.

4. Conclusion

Fracture toughness is one of the most important properties of any material for a lot of design applications involving damage and crack growth. Unfortunately its value can be difficult to evaluate with standard methods such as “compliance” method. Hence, in this study we propose linking the fracture toughness to the experimental heat sources [13]. In this way, the fracture toughness can be computed even for experiments where the stiffness variation remains small.

Damage of compressive fiber failure in unidirectional composite laminate has been chosen for its difficulty to evaluate toughness. The infrared has been used to follow compressive failure mode developing during an indentation test and a compression after impact test, and to evaluate the fracture toughness of compressive fiber failure. The average values of G_{Ic}^{comp} , for static indentation test and CAI test are **32.6** N/mm and **42.5** N/mm, respectively. These obtained results are well corresponding to the value found in previous work [8] (40 N/mm) from FE analysis of impact damage and are coherent with literature [1, 14].

References

[1] Pinho ST, Robinson P, Iannucci L., Fracture toughness of the tensile and compressive fibre failure modes in laminated composites, Compos. Sci. Tech., Vol. 66, pp. 2069-2079, 2006.

[2] Chrysochoos A, Louche H. An infrared image processing to analyse the calorific effects accompanying strain localisation. Int J. Eng Sci, Vol. 38, pp. 1759-88, 2000.

[3] Dumoulin S, Louche H, Hopperstad O, Borvik T., Heat sources, energy storage and dissipation in high-strength steels: experiments and modeling, Eur. J. Mech. A/Solids, Vol. 29, pp. 461-74, 2010.

[4] Wattrisse B, Muracciole JM, Chrysochoos A., Thermomechanical effects accompanying the localized necking of semi-crystalline polymers, Int. J. Therm. Sci., Vol. 41(5), pp. 422-7, 2002.

[5] Chrysochoos A, Chezeaux JC, Caumon H., Analyse thermomecanique des lois de comportement par thermographie infrarouge, Rev. Phys. Appl., Vol. 24(2), pp. 215-25, 1989.

[6] Naderi M, Kahirdeh A, Khonsari M., Dissipated thermal energy and damage evolution of glass/epoxy using infrared thermography and acoustic emission, Compos. Part B: Eng. Vol. 43(3), pp. 1613-20, 2012.

[7] Rice J., A path independent integral and the approximate analysis of strain concentration by notches and cracks, J. Appl. Mech., Vol. 35, pp. 379-86, 1968.

[8] Freund L., Hutchinson J., High strain-rate crack growth in rate-dependent plastic solids, J. Mech. Phys. Solids, Vol. 33(2), pp. 169-91, 1985.

[9] Soumahoro Z., Etude du couplage thermomécanique dans la propagation dynamique de fissure, Ph.D. thesis, Ecole Polytechnique; 2005.

[10] Taylor GI, Quinney H., The latent energy remaining in a metal after cold working, Proc. Roy. Soc. Part A, Vol. 143(849), pp. 307-26, 1934.

[11] Kapoor R, Nemat-Nasser S., Determination of temperature rise during high strain rate deformation, Mech. Mater., Vol. 27(1), pp. 1-12, 1998.

[12] Li Z, Lambros J., Strain rate effects on the thermomechanical behavior of polymers, Int. J. Solids Struct., Vol. 38(20), pp. 3549-62, 2001.

[13] Lisle T., Bouvet C., Pastor M.L., Margueres P., Prieto Corral R., Damage analysis and fracture toughness evaluation in a thin woven composite laminate under static tension using infrared thermography, Compos. Part A, Vol. 53, pp. 75-87, 2013.

[14] Soutis C, Curtis PT. A method for predicting the fracture toughness of CFRP laminates failing by fibre microbuckling. Compos Part A: Appl Sci Manuf 2000;31:733–40.

[15] Hongkarnjanakul N, Bouvet C, Rivallant S. Validation of low velocity impact modelling on different stacking sequences of CFRP laminates and influence of fibre failure. Compos Struct 2013;106:549–59.

[16] Rivallant S., Bouvet C., Abi Abdallah E., Broll B., Barrau J.J., Experimental analysis of CFRP laminates subjected to compression after impact: the role of impact-induced cracks in failure, Composite Structures 2014, Vol. 111, pp. 147-57